Int. J. Electron. Commun. (AEÜ) 66 (2012) 605–612

Contents lists available at SciVerse ScienceDirect

International Journal of Electronics and Communications (AEÜ)

journal homepage: www.elsevier.de/aeue

Distributed antenna network for gigabit wireless access

Fumiyuki Adachi *, Wei Peng, Tatsunori Obara, Tetsuya Yamamoto, Ryusuke Matsukawa, Masayuki Nakada

Department of Electrical and Communication Engineering, Graduate School of Engineering, Tohoku University 6-6-05, Aza-aoba, Aramaki, Aoba-ku, Sendai 980-8579, Japan

ARTICLE INFO

Article history:
Received 4 November 2011
Accepted 16 March 2012

Keywords:
Distributed antenna network
Single-carrier
Frequency-domain equalization
Relay
Beamforming
Multiplexing

ABSTRACT

For gigabit wireless data services, there are three important technical issues to be addressed: limited bandwidth, severe frequency-selective fading, and limited transmit power. A distributed antenna network (DAN) is a promising solution to the above three technical issues. In DAN, each mobile user is served by using multiple distributed antennas close to it. In this paper, recent advances in various distributed multi-input/multi-output (MIMO) techniques combined with single-carrier (SC) frequency-domain signal processing are presented for DAN. Particular attention is paid to SC frequency-domain MIMO diversity, relay, beamforming, and multiplexing jointly used with frequency-domain equalization (FDE) to significantly improve the signal transmission performance.

1. Introduction

The 3rd generation long term evolution (LTE) systems with a peak data rate of few hundreds Mbps are now deployed in many countries [1]. A next step is the development of broadband (gigabit) wireless technology to be used in the 4th generation systems with a peak data rate of around 1 Gbps. There will be three important technical issues to be addressed: severe frequency-selective fading, limited transmit power, and limited bandwidth. The gigabit wireless channel is severely frequency-selective and severe intersymbol interference (ISI) is produced. Frequency-domain signal processing, e.g., frequency-domain equalization (FDE) [2,3], may play an important role in achieving a good signal transmission performance in such a severe frequency-selective channel. In addition to the above, the path loss and shadowing loss cause a severe received signal power drop since the transmit power is limited. Gigabit data services are available only near the base station (BS) if the present wireless network architecture is employed with limited transmit power. A distributed antenna network (DAN) [4], in which many antennas are distributed over a service area, is a promising solution to the above three technical issues.

The concept of DAN is illustrated in Fig. 1. In DAN, the conventional BS is replaced by the signal processing center (SPC) and many antennas or clusters of antennas are spatially distributed over the service area so that some antennas can always be visible from a mobile terminal (MT) with a high probability. Antennas or antenna clusters are connected to nearby SPC by means of optical fiber links or wireless links. It is desirable to use as many distributed antennas as possible while the number of MT antennas is limited to one or two since there is not enough space to equip too many antennas at an MT. A number of distributed antennas cooperate and act as distributed multiple-input multiple-output (MIMO) diversity, relay, beamforming, or multiplexing.

For the DAN downlink, either the single-carrier (SC) or multi-carrier (MC) transmission can be used. However, for the uplink transmission, SC is promising since it has a lower peak-to-average power ratio (PAPR). Using a transmit power amplifier with the same peak power, SC provides longer communication range than MC. Therefore, we have been investigating a potentiality of SC-DAN [4]. In this paper, recent advances in various distributed MIMO transmission techniques combined with SC frequency-domain signal processing are presented for DAN. Particular attention is paid to SC frequency-domain MIMO transmission techniques, i.e., antenna diversity, relay, beamforming, and multiplexing, to significantly improve the transmission performance. It is quite difficult if not impossible to deal with the above technical issues theoretically. Therefore, in this paper, we resort to the computer simulation method to evaluate the performances achievable with SC frequency-domain MIMO signal transmission techniques. This paper provides a comprehensive performance evaluation of DAN by computer simulation.

The rest of the paper is organized as follows. In Section 2, distributed MIMO diversity implemented by the frequency-domain space-time coded joint transmit/receive diversity (FD-STBC-JTRD) combined with transmit FDE is presented. Section 3 presents the distributed cooperative amplify-and-forward (AF)

* Corresponding author. Tel.: +81 22 795 7082; fax: +81 22 795 7083.
E-mail address: adachi@ecei.tohoku.ac.jp (F. Adachi).

1434-8411/$ – see front matter © 2012 Elsevier GmbH. All rights reserved.
doi:10.1016/j.aeue.2012.03.010

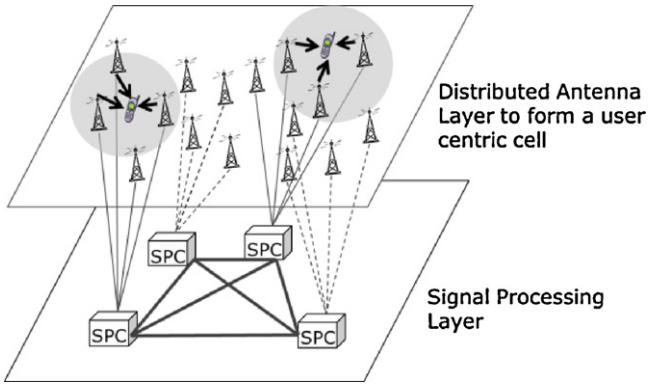

Fig. 1. Concept of DAN.

relay. Distributed beamforming and spatial multiplexing are discussed in Sections 4 and 5, respectively. Some concluding remarks are drawn in Section 6.

2. Distributed MIMO diversity

For the downlink, frequency-domain space-time block coded joint transmit/receive diversity (FD-STBC-JTRD) combined with transmit FDE [5] can be used. It allows the use of an arbitrary number N_{dan} of distributed transmit antennas while the number of MT receive antennas is limited to $N_{mt} \leq 6$. Note that for the uplink, frequency-domain space time transmit diversity (FD-STTD) [6] is promising since it allows the use of an arbitrary number N_{dan} of distributed receive antennas. A combination of FD-STBC-JTRD for downlink and FD-STTD for uplink is suitable for DAN.

Fig. 2 illustrates the transmitter/receiver structures using FD-STBC-JTRD for the downlink packet access with turbo-coded hybrid automatic repeat request (HARQ) using type-II S-P2 strategy [7]. The FD-STBC-JTRD is applied to a sequence of J blocks of N_c symbols each to generate N_{dan} streams of Q encoded blocks. A combination of J and Q is found in [5]. The transmit symbol matrix $\mathbf{S}(k)$ of size $N_{dan} \times Q$ at the kth frequency can be expressed as

$$\mathbf{S}(k) = C_{N_{mt}} \mathbf{W}^H(k) \mathbf{D}_{N_{mt}}(k), \tag{1}$$

where $\mathbf{W}^H(k)$ and $\mathbf{D}_{N_{mt}}(k)$ represent the transmit FDE matrix of size $N_{dan} \times N_{mt}$ having $W_{m,n}(k)$ as its (m, n)th entity and the STBC-JTRD encoding matrix of size $N_{mt} \times Q$, respectively. $C_{N_{mt}} = \left\{ N_c / \sum_{k=0}^{N_c-1} \sum_{m=0}^{N_{mt}-1} \sum_{n=0}^{N_{dan}-1} \left| W_{m,n}(k) \right|^2 \right\}^{1/2}$ is the power normalization coefficient. $\mathbf{W}(k)$ is given by

$$\mathbf{W}(k) = A(k) \cdot \mathbf{H}(k), \tag{2}$$

where $\mathbf{H}(k)$ is the channel matrix of size $N_{mt} \times N_{dan}$ having $H_{m,n}(k)$ as its (m, n)th entity, and $A(k)$ is the scaling factor. Assuming minimum mean square error (MMSE) transmit FDE, $A(k)$ is given by

$$A(k) = \frac{1}{(1/N_{mt}) \sum_{m=0}^{N_{mt}-1} \sum_{n=0}^{N_{dan}-1} \left| H_{m,n}(k) \right|^2 + ((E_s/N_0))^{-1}}, \tag{3}$$

where E_s and N_0 are the symbol energy and single-sided power spectrum density of additive white Gaussian noise (AWGN), respectively. $\mathbf{D}_{N_{mt}}(k)$ for different values of N_{mt} can be found in [5]. When $N_{mt} = 2$ and $Q = 2$, we have

$$\mathbf{D}_{N_{mt}=2}(k) = \begin{pmatrix} D_0(k) & -D_1^*(k) \\ D_1(k) & D_0^*(k) \end{pmatrix}. \tag{4}$$

$\{\mathbf{S}(k); k = 0 \sim N_c - 1\}$ are transformed by an N_c-point inverse fast Fourier transform (IFFT) into the time-domain N_{dan} streams of Q encoded blocks to be transmitted from N_{dan} distributed antennas.

The received signals on N_{mt} receive antennas at MT can be expressed in frequency domain as

$$\mathbf{R}(k) = \sqrt{2P_t} \mathbf{H}(k) \mathbf{S}(k) + \mathbf{N}(k), \tag{5}$$

where $\mathbf{R}(k)$ represents the frequency-domain received signal matrix of size $N_{mt} \times Q$, $\mathbf{N}(k)$ represents the noise matrix of size $N_{mt} \times Q$, whose elements are i.i.d. zero-mean complex Gaussian variables having variance $2N_0/T_s$ with T_s being the symbol length, and $P_t = E_s/T_s$ denotes the total transmit power. The frequency-domain received signal vector $\hat{\mathbf{D}}_{N_{mt}}(k)$ after FD-STBC-JTRD decoding [5] can be expressed in the vector form as

$$\hat{\mathbf{D}}_{N_{mt}}(k) = \sqrt{2P_t} A(k) \left(\sum_{m=0}^{N_{mt}-1} \sum_{n=0}^{N_{dan}-1} \left| H_{m,n}(k) \right|^2 \right) \begin{pmatrix} D_0(k) \\ \vdots \\ D_{J-1}(k) \end{pmatrix} + \hat{\mathbf{N}}(k), \tag{6}$$

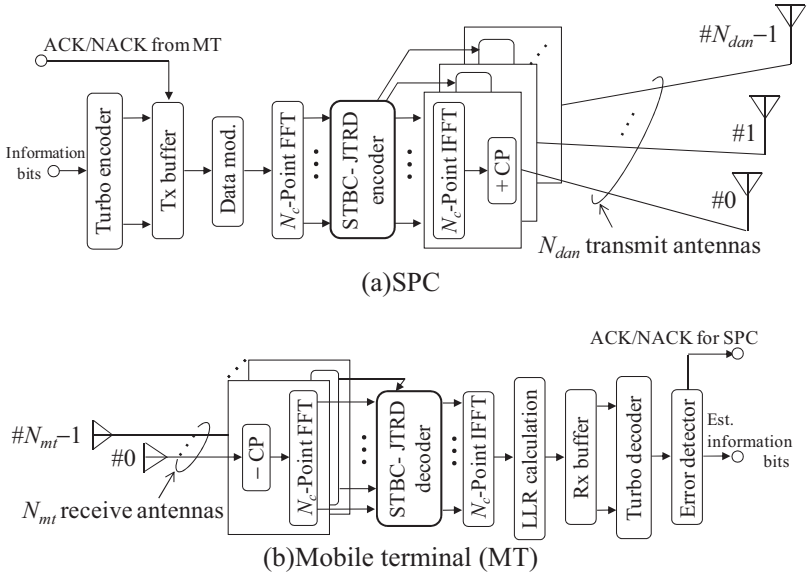

Fig. 2. Transmitter/receiver structures of FD-STBC-JTRD downlink. (a)SPC. (b)Mobile terminal (MT).

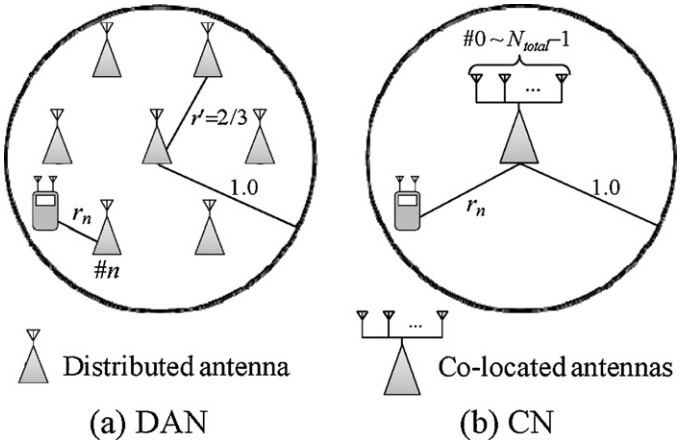

Fig. 3. Models of DAN and CN. (a) DAN (b) CN.

where $\hat{\mathbf{N}}(k)$ represents the noise vector whose elements are i.i.d. zero-mean complex Gaussian variables having variance $2N_{mt}N_0/T_s$. It can be understood from Eq. (6) that FD-STBC-JTRD achieves the $N_{mt} \times N_{dan}$-order diversity. The time-domain soft decision symbol vector is obtained by applying N_c-point IFFT to $\{\hat{\mathbf{D}}_{N_{mt}}(k); k = 0 \sim N_c - 1\}$.

Computer simulations are done to measure the throughput distributions of DAN and a conventional cellular network (CN), both of which use FD-STBC-JTRD. Fig. 3 illustrates the models of DAN and CN. $N_{total} = 7$ antennas are assumed. In the case of the DAN, 6 antennas are equidistantly distributed along a circle of normalized radius $r' = 2/3$ and one antenna is located the center of cell. N_{dan} antennas are selected from $N_{total} = 7$ antennas, based on the local average received signal power (i.e., the antenna selection is based on the path loss plus shadowing loss). On the other hand, in the case of the CN, N_{dan} antennas are selected from N_{total} antennas co-located at the BS, based on the instantaneous received signal power.

The downlink packet access using Rate-1/3 turbo coded HARQ using type-II S-P2 strategy [7] is computer simulated. 16QAM data modulation, $N_c = 256$, and $N_g = 32$ are assumed. A packet is composed of 1536 information bits. Rate-1/3 turbo coded type-II S-P2 strategy uses three bit sequences of equal length: the systematic bit sequence, the first interleaved parity bit sequence, and the second interleaved parity bit sequence. First, only the systematic bit sequence is transmitted. If any errors are detected, the first parity bit sequence is transmitted. Still any errors are detected, the second parity bit sequence is transmitted. The above transmission process

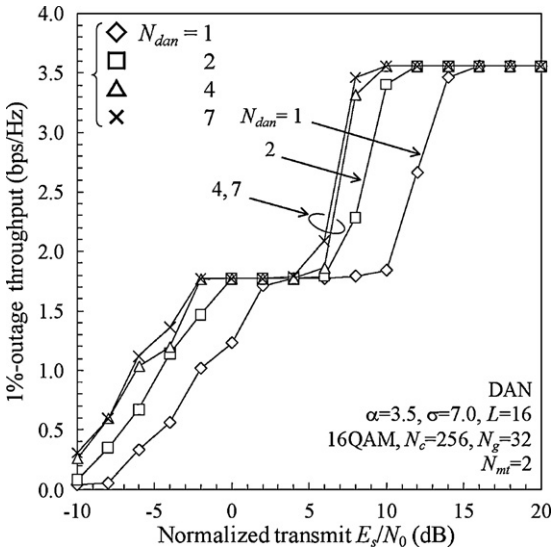

Fig. 5. 1%-outage throughput. (a) DAN (b) CN.

is repeated until the packet is correctly received by MT. An $L = 16$-path frequency-selective block Rayleigh fading channel is assumed. Fading is assumed to stay unchanged over the transmission of each packet (either systematic bit sequence, first parity bit sequence, or second parity bit sequence), but changes packet-by-packet. The throughput is measured by changing the MT's location randomly to find the cumulative distribution function (CDF). The shadowing and path losses are changed only when the MT's location is changed.

The spatial distribution of the measured throughput in DAN and CN is illustrated in Fig. 4 for $(N_{dan}, N_{mt}) = (4,2)$ and the normalized transmit $E_s/N_0 = 0$ dB. It can be clearly seen from Fig. 4 that DAN achieves much higher throughput in a cell. In the CN, all the antennas suffer from the same path loss and shadowing loss and therefore, the throughput at the cell edge significantly drops. The throughput at the cell edge is about 2.6 (bps/Hz) in DAN while it is about 1.2 (bps/Hz) in CN. Fig. 5 plots the 1%-outage throughput, which is the 1% value of the CDF, with N_{dan} as a parameter for DAN. It can be seen from Fig. 5 that increasing N_{dan} achieves higher throughput due to its larger spatial diversity gain. By increasing N_{dan} from 1 to 4, the transmit power can be reduced by about 6 dB. However, the use of more than $N_{dan} = 4$ provides only a marginal increase in the throughput. This is because as N_{dan} increases, more antennas which are not close to MT are selected. They do not

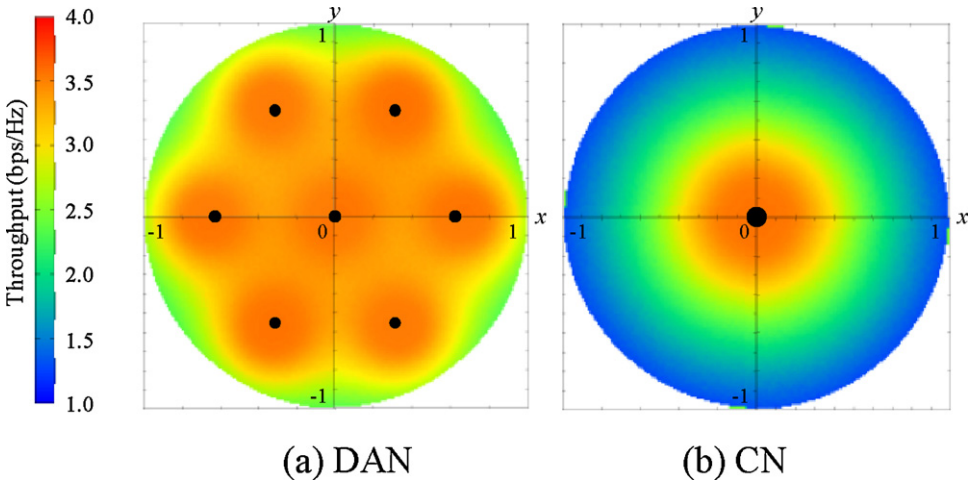

Fig. 4. Spatial distribution of throughput ($N_{total} = 7$ antennas and 16QAM data modulation).

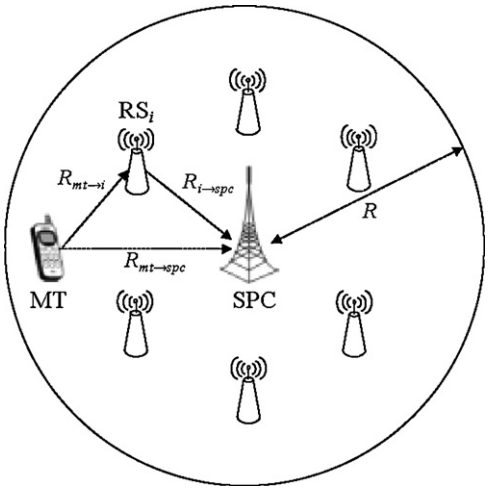

Fig. 6. Cooperative AF relay.

contribute to the performance improvement since most part of total transmit power is allocated to antennas close to the MT.

3. Distributed cooperative relay

The cooperative amplify-and-forward (AF) relay using 2-time slots [8] is a powerful means to extend the coverage with limited MT transmit power. Each distributed antenna is replaced by relay stations (RSs). Fig. 6 illustrates a DAN with 6 distributed RSs and SPC equipped with the single antenna. The cell radius is denoted by R. The distances between MT and SPC, between MT and the ith RS (denoted by RS$_i$), and between the RS$_i$ and SPC are denoted by $R_{mt\to spc}$, $R_{mt\to i}$, and $R_{i\to spc}$, respectively. MT is assumed to have the single antenna ($N_{mt}=1$). The best RS ($N_{dan}=1$) which provides the maximum channel capacity is selected from 6 RSs. In the first time slot, MT broadcasts to SPC and RS; in the second time-slot, RS transmits an amplified version of its received signal to SPC.

SC uplink block transmission of N_s symbols per block is considered. A total number N_c ($>N_s$) of subcarriers used in the system are divided into N_c/N_b resource blocks of N_b consecutive subcarriers each. It is assumed that an MT transmits an N_s-symbol block to SPC. Spectrum division/adaptive subcarrier allocation (SDASA) [9] is considered. The frequency-domain signal of N_s-symbol block to be transmitted is divided into $D=N_s/N_b$ sub-blocks of N_b frequency components each. They are adaptively mapped onto D different resource blocks based on the channel conditions of MT–RS–SPC and MT–SPC links to achieve the maximum channel capacity. An example of SDASA with $(N_c, N_b, N_s)=(16, 2, 8)$ is illustrated in Fig. 7.

Relaying is not always effective. Sometimes, the direct communication provides higher capacity. In the direct/cooperative AF relay (D/AR) switching, the cooperative AF relay is used only if it provides larger channel capacity than the direct communication. The channel capacity C^{sw} of the D/AR switching using SDASA is expressed as

$$C^{sw}=\max\{C^{dc}, C_i^{cr}\}, \tag{7}$$

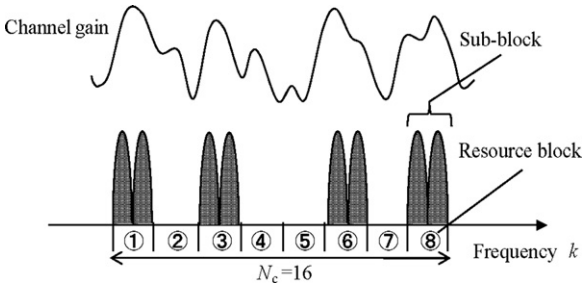

Fig. 7. An example of SDASA when $(N_c, N_b, N_s)=(16, 2, 8)$.

where C^{dc} and C_i^{cr} are the channel capacities for the direct communication and the cooperative AF relay using RS$_i$, respectively. The channel capacity C^{dc} for the direct communication is given by [10]

$$C^{dc}=\frac{1}{N_s}\sum_{k=0}^{N_c-1}\varepsilon_k^{dc}\log_2\left(1+\frac{P_r^{dc}}{N_{spc}}|H_{mt\to spc}(k)|^2\right), \tag{8}$$

where $H_{mt\to spc}(k)$ and N_{spc} are respectively the channel gain for the MT–SPC link and the noise power at SPC. P_r^{dc} is the received signal power at SPC and is given as

$$P_r^{dc}=\bar{P}_T\cdot r_{mt\to spc}^{-\alpha}\cdot 10^{-\eta/10}, \tag{9}$$

where $\bar{P}_T=P_T\cdot R^{-\alpha}$ is the normalized MT transmit power with P_T being the MT transmit power and α being the path loss exponent, $r_{mt\to spc}=R_{mt\to spc}/R$ is the normalized distance between MT and SPC, and η is the shadowing loss in dB. ε_k^{dc} takes 0 or 1 ("$\varepsilon_k^{dc}=1$" indicates that the kth subcarrier is used on the MT–SPC link and 0 otherwise).

The channel capacity C_i^{cr} of the cooperative AF relay using RS$_i$ is given by [10]

$$C_i^{cr}=\frac{1}{2}\sum_{k=0}^{N_c-1}\sum_{k'=0}^{N_c-1}\frac{\varepsilon_{i,k,k'}^{cr}}{N_s}\log_2\left(1+\frac{P_{r,mt\to spc}^{cr}}{N_{spc}}\left|H_{mt\to spc}(k)\right|^2+\frac{(P_{r,mt\to i}^{cr}/N_{RS_i})\left|H_{mt\to i}(k)\right|^2\cdot(P_{r,i\to spc}^{cr}/N_{spc})\left|H_{i\to spc}(k')\right|^2}{(P_{r,mt\to i}^{cr}/N_{RS_i})\sum_{j=0}^{N_c-1}\sum_{j'=0}^{N_c-1}(\varepsilon_{i,j,j'}^{cr}/N_s)\left|H_{mt\to i}(j)\right|^2+(P_{r,i\to spc}^{cr}/N_{spc})\left|H_{i\to spc}(k')\right|^2+1}\right), \tag{10}$$

where $H_{mt\to i}(k)$ and $H_{i\to spc}(k)$ are the channel gain for the MT–RS$_i$ link and the RS$_i$–SPC link, respectively. N_{RS_i} is the noise power at RS$_i$. $P_{r,mt\to spc}^{cr}$, $P_{r,mt\to i}^{cr}$ and $P_{r,i\to spc}^{cr}$ are respectively the received signal powers at SPC and RS$_i$ in the first time slot and SPC in the second time slot and are given as $P_{r,mt\to spc}^{cr}=\bar{P}_{t,mt}\cdot r_{mt\to spc}^{-\alpha}\cdot 10^{-\eta/10}$, $P_{r,mt\to i}^{cr}=\bar{P}_{t,mt}\cdot r_{mt\to i}^{-\alpha}\cdot 10^{-\eta/10}$, and $P_{r,i\to spc}^{cr}=\bar{P}_{t,i}\cdot r_{i\to spc}^{-\alpha}\cdot 10^{-\eta/10}$, where $\bar{P}_{t,mt}=P_{t,mt}\cdot R^{-\alpha}$ and $\bar{P}_{t,i}=P_{t,i}\cdot R^{-\alpha}$ are respectively the normalized MT transmit power with $P_{t,mt}$ being the MT transmit power and the normalized RS$_i$ transmit power with $P_{t,i}$ being the RS$_i$ transmit power. $r_{mt\to i}=R_{mt\to i}/R$ and $r_{i\to spc}=R_{i\to spc}/R$ are the normalized distances. $\varepsilon_{i,k,k'}^{CR}$ in Eq. (10) takes 0 or 1 ("$\varepsilon_{i,k,k'}^{CR}=1$" indicates that the kth subcarrier and k'th subcarrier are respectively used in the first and second time slots, and 0 otherwise). For the fair performance comparison between cooperative relay and direct communication, the MT transmit power of direct communication is assumed to have the same total transmit power given by $\bar{P}_T=\bar{P}_{t,mt}+\bar{P}_{t,i}$.

The channel capacity of the D/AR switching using SDASA is measured by computer simulation. 6 RSs are distributed equidistantly along a circle of the normalized radius 2/3 ($r_{i\to spc}=2/3$) similar to Fig. 3. Fig. 8 shows the spatial distribution of the 10%-outage capacity of the D/AR switching (note that SDASA is not used). 6 RSs and SPC are respectively illustrated by black dots and triangle. It can be seen from Fig. 8 that the D/AR switching can achieve larger 10%-outage capacity than the direct communication and the cooperative AF relay over an entire area. When the D/AR switching is used, the

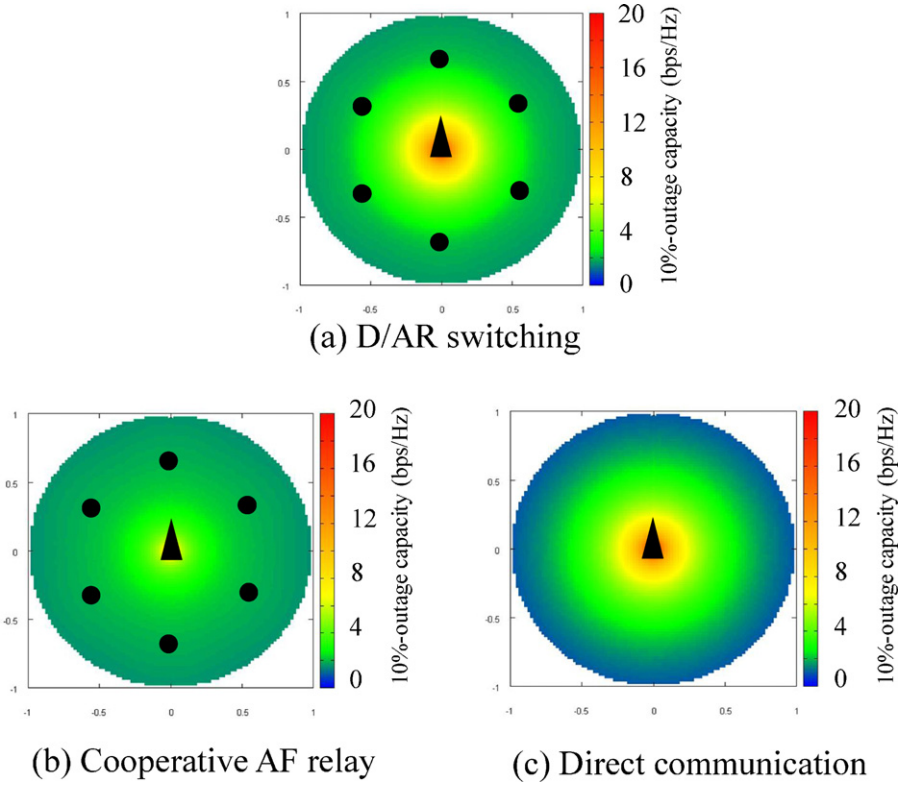

Fig. 8. Spatial distribution of the 10%-outage capacity. (a) D/AR switching. (b) Cooperative AF relay. (c) Direct communication.

10%-outage capacity is 1.6(19.0) bps/Hz at the cell age (at the center of the cell) while it is about 0.9(19.0) bps/Hz and 1.5(9.0) bps/Hz when the direct communication and the cooperative AF relay are used, respectively.

The throughput is measured by changing the MT's location randomly to find the CDF of the channel capacity. Fig. 9 plots the 10%-outage capacity, computed from the CDF, of the D/AR switching without SDASA as a function of the normalized transmit power-to-noise power ratio (SNR) $\Gamma_i = \bar{P}_T/N$. The D/AR switching can reduce the transmit power compared to the direct communication and the cooperative AF relay. The transmit power required for achieving a 10%-outage capacity of 1.0 bps/Hz can be reduced by about 3 dB compared to the direct communication and by about 1 dB compared to the cooperative AF relay. An additional use of SDASA obtains the frequency diversity gain and can further reduce the required transmit power compared to the D/AR switching without SDASA. This is clearly seen from Fig. 10 which plots the 10%-outage capacity of the D/AR switching jointly used SDASA.

4. Distributed beamforming

The SC beamforming implemented by frequency-domain adaptive antenna array (FDAAA) [11] is effective to improve the received signal power while suppressing own signal ISI and the other users' co-channel interference (CCI) [4]. Distributed clusters of antennas shown in Fig. 11 are considered. 7 antenna clusters are equidistantly distributed along a circle of normalized radius (2/3)R and one antenna cluster is located at the center of cell, where each antenna

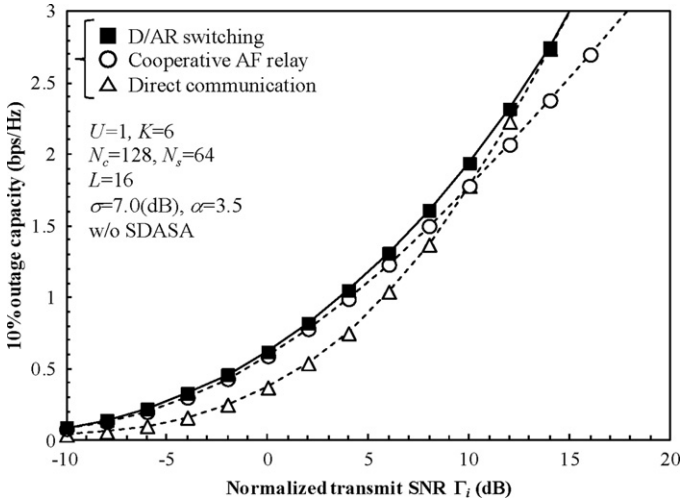

Fig. 9. 10%-outage capacity of D/AR switching.

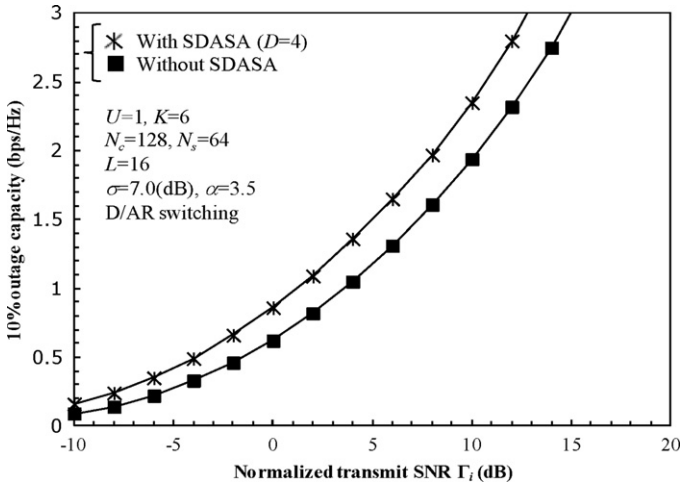

Fig. 10. Additional capacity improvement by SDASA.

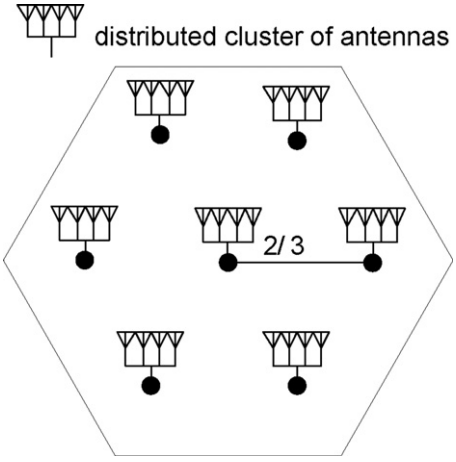

Fig. 11. Distributed cluster of antennas.

cluster consists of N_r antennas with linear array configuration. Four frequency reuse patterns shown in Fig. 12 are considered.

Uplink performance of the distributed beamforming in DAN system are investigated by computer simulations assuming single cell environment and cellular environment with the frequency reuse factor (FRF) = 1, 3, 4 and 7. It is assumed that each distributed cluster has 4 antennas. Scheduling among clusters of antennas is considered and up to two (D = 1, 2) active clusters of antennas are used. The cluster(s) of antennas which have shortest distance(s) to the desired user will be used. The weight control is performed on the received signals of each cluster of antennas, given by

$$\tilde{R}(k) = \mathbf{W}^T(k)\mathbf{R}(k), \tag{11}$$

where $\mathbf{R}(k) = [R_0(k), \ldots, R_n(k), \ldots, R_{N_r-1}(k)]^T$ is the frequency domain received signal vector with $R_n(k)$ representing the received signal at the kth frequency on the nth antenna, $n = 0 \sim N_r - 1$, and $\mathbf{W}(k) = [W_0(k), \ldots, W_{N_r-1}(k)]$ is the beamforming weight vector.

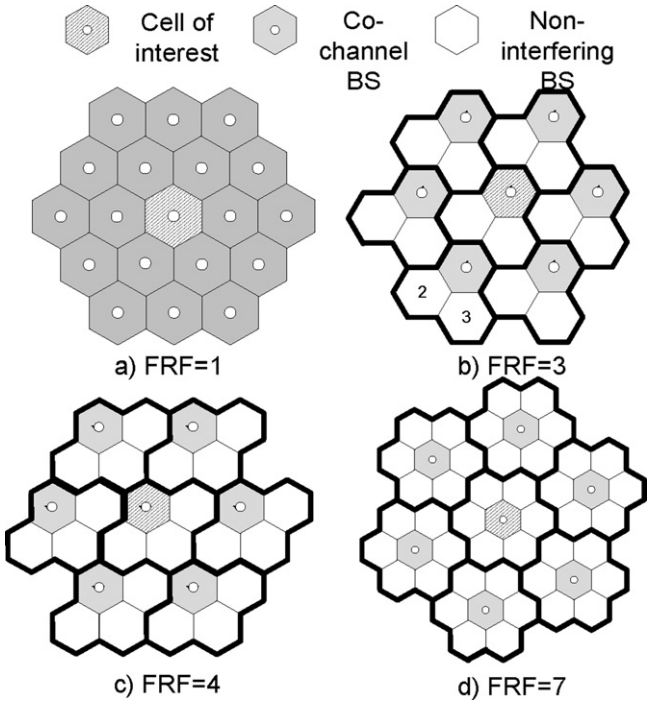

Fig. 12. Cellular structure.

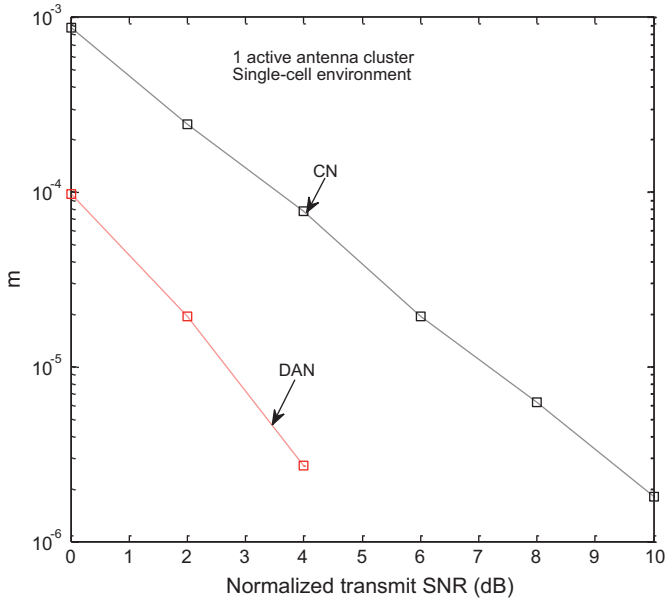

Fig. 13. 10% outage BER in single-cell environment.

Computer simulations are done to measure the uplink bit error rate (BER) in a single-cell environment and in a multi-cell environment with frequency reuse. The 10%-outage BER is plotted for the 1 active antenna cluster case in Fig. 13 as a function of the normalized transmit signal-to-noise ratio (SNR). In order to see whether the beamforming technique can benefit from the distributed nature of DAN, the 10%-outage BER of CN is also plotted in Fig. 13. In order to make fair comparison, the number of antennas of CN is set to be equal to the total number of distributed antennas in use. It can be observed that distributed beamforming in DAN can reduce the 10% outage BER significantly compared to CN.

The 10% outage BER in a multi-cell environment is plotted in Fig. 14. It can be observed that beamforming in DAN is more robust to the CCI. Even with FRF = 1 (strong CCI exists), better quality of communication can be realized by using the distributed beamforming compared to the CN case. Due to the increased diversity order,

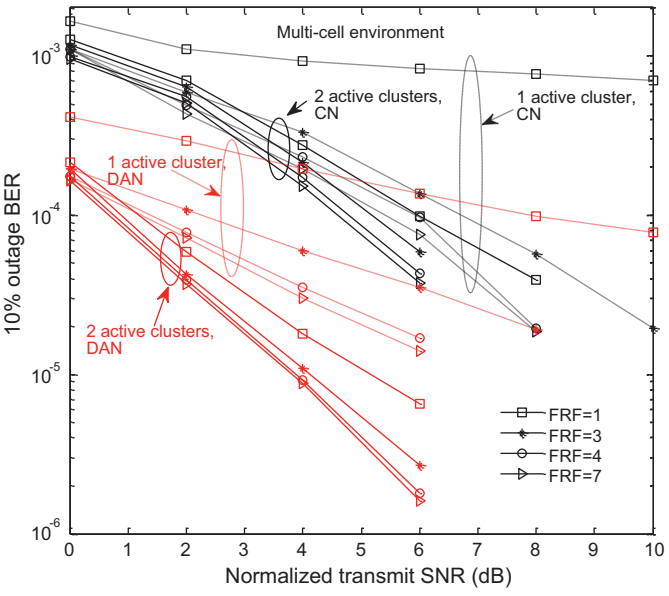

Fig. 14. 10% outage BER in a multi-cell environment.

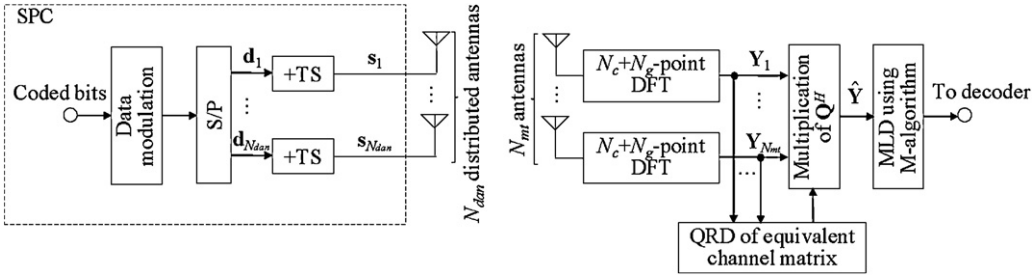

Fig. 15. TS-SC MIMO multiplexing using QRM-MLBD.

the 10% outage BER performance with 2 active antenna clusters is much better than the one with 1 active antenna cluster.

In this study, perfect synchronization has been assumed and how to synchronize the active antenna clusters remains as our future work.

5. Distributed multiplexing

Multiple distributed antennas in DAN can be used not only for spatial diversity but also for the spatial multiplexing to improve the throughput [12]. The downlink transmission is considered below. N_{dan} different antennas are selected from N_{total} distributed antennas and simultaneously used for spatial multiplexing. A training-sequence (TS) aided SC (TS-SC) and maximum likelihood (ML) block signal detection using QR decomposition and M-algorithm (QRM-MLBD) [13] is considered.

TS-SC MIMO multiplexing using QRM-MLBD is illustrated in Fig. 15. The data-modulated symbol sequence to be transmitted is serial-to-parallel (S/P) converted to N_{dan} parallel symbol sequences, each parallel symbol sequence is divided into a sequence of symbol blocks of N_c symbols each. Before the transmission, the TS of length N_g symbols is appended at the end of each block. The block $\mathbf{s}_n = [s_n(0),\ldots,s_n(t),\ldots,s_n(N_c+N_g-1)]^T$ $([.]^T$ representing the transposition) to be transmitted from the nth antenna is expressed using the vector form as $\mathbf{s}_n = [\mathbf{d}_n^T \mathbf{u}_n^T]^T$, where $\mathbf{d}_n = [d_n(0),\ldots,d_n(t),\ldots,d_n(N_c-1)]^T$ is the data symbol vector and $\mathbf{u}_n = [u_n(0),\ldots,u_n(t),\ldots,u_n(N_g-1)]^T$ is the TS vector which is identical for all blocks.

In order to let TS to play the role of cyclic prefix (CP), the discrete Fourier transform (DFT) size to be used at the receiver must be N_c+N_g symbols (the sum of data block length and TS in symbols). The use of TS instead of CP can reduce the required number of surviving paths in the M-algorithm. At the MT, QRM-MLBD is applied to the overall frequency-domain received signal by treating a concatenation of the space and frequency-domain channel and DFT as the equivalent channel. The $N_{mt}N_c \times 1$ frequency-domain received signal $\mathbf{Y}_{all} = \left[\{\mathbf{Y}_1\}^T \cdots \{\mathbf{Y}_{N_{mt}}\}^T\right]^T$ with $\mathbf{Y}_m$ representing the frequency-domain received signal vector at the mth receive antenna is given by [13]

$$\begin{aligned}\mathbf{Y}_{all} &= \sqrt{\frac{2E_s}{T_s}}\begin{bmatrix}\mathbf{H}_{1,1}\mathbf{F} & \cdots & \mathbf{H}_{1,N_{dan}}\mathbf{F}\\ \vdots & \ddots & \vdots\\ \mathbf{H}_{N_{mt},1}\mathbf{F} & \cdots & \mathbf{H}_{N_{mt},N_{dan}}\mathbf{F}\end{bmatrix}\begin{bmatrix}\mathbf{s}_1\\ \vdots\\ \mathbf{s}_{N_{dan}}\end{bmatrix}+\begin{bmatrix}\mathbf{N}_1\\ \vdots\\ \mathbf{N}_{N_{mt}}\end{bmatrix},\\ &= \sqrt{\frac{2E_s}{T_s}}\mathbf{H}\mathbf{s}_{all}+\mathbf{N}_{all}\end{aligned} \tag{12}$$

where $\mathbf{H}_{m,n}$ denotes the frequency-domain channel matrix between the nth transmit antenna and mth receive antenna, $\mathbf{F}$ the DFT matrix of size $(N_c+N_g)\times(N_c+N_g)$, $\mathbf{N}_m$ the frequency-domain noise vector. In the second equation of Eq. (12), $\mathbf{H}$ denotes an equivalent channel matrix of size $N_{mt}(N_c+N_g)\times N_{dan}(N_c+N_g)$, which is a concatenation of the space and frequency-domain channel and DFT, $\mathbf{s}_{all}$ the overall transmit symbol vector of size $N_{dan}(N_c+N_g)\times 1$, and $\mathbf{N}_{all}$ denotes the overall noise vector of size $N_{mt}(N_c+N_g)\times 1$.

QRM-MLBD consists of three steps: ordering (TSs are moved to the bottom of the vector), QR decomposition, and M-algorithm. The overall transmit symbol vector $\mathbf{s}^{order} = [s_1(0),\ldots,s_{N_t}(0),\ldots,s_1(N_c+N_g-1),\ldots,s_{N_t}(N_c+N_g-1)]^T$ after ordering is expressed as

$$\mathbf{s}^{order} = [\mathbf{d}^T(0),\mathbf{d}^T(1),\ldots,\mathbf{d}^T(N_c-1),\mathbf{u}^T(0),\ldots,\mathbf{u}^T(N_g-1)]^T, \tag{13}$$

where $\mathbf{d}^T(t)$ and $\mathbf{u}^T(t)$ denote the data symbol vector and TS vector at tth symbol of size $N_t\times 1$, respectively. After ordering, the QR decomposition is applied to the ordered equivalent channel matrix $\mathbf{H}$ to obtain $\mathbf{H}=\mathbf{QR}$, where $\mathbf{Q}$ is an $N_{mt}(N_c+N_g)\times N_{dan}(N_c+N_g)$ unitary matrix and $\mathbf{R}$ is an $N_{mt}(N_c+N_g)\times N_{dan}(N_c+N_g)$ upper triangular matrix. The transformed frequency-domain received signal $\hat{\mathbf{Y}} = [\hat{Y}(1),\ldots,\hat{Y}(N_{dan}(N_c+N_g))]^T$ is obtained as

$$\hat{\mathbf{Y}} = \mathbf{Q}^H\mathbf{Y}_{all} = \sqrt{\frac{2E_s}{T_s}}\mathbf{R}\mathbf{s}^{order}+\mathbf{Q}^H\mathbf{N}_{all}. \tag{14}$$

The MLD can be converted to the successive tree search problem and the computational complexity can be reduced by introducing the M-algorithm [14] into the successive tree search. In the case of SC-MIMO block transmissions, the magnitude of a complex-valued element closer to the lower right positions of matrix $\mathbf{R}$ may drop with higher probability. The received signal powers associated with symbols to be detected at early stages in the M-algorithm significantly drop and hence, the probability of removing the correct path at early stages may increase when a smaller number M of surviving paths is used. In TS-SC MIMO multiplexing with ordering, the symbols to be detected at early stages in the M-algorithm are symbols belonging to the known TSs. Therefore, the probability of removing the correct path can be significantly reduced.

Computer simulation is done to measure the throughput distributions of DAN and CN, both using $N_{total}=7$. The same antenna distribution pattern as in Section 3 is assumed. The single-user and single-cell SC-DAN is considered. Antenna selection is based on the local average received signal power. TS-SC MIMO multiplexing ($N_c=64$ and $N_g=16$) using QRM-MLBD. Turbo-coded HARQ type-II S-P4 strategy [7], and 16QAM are considered. Packet size is 2048. The number M of surviving paths in the M-algorithm is set to 16. An $L=16$-path frequency-selective block Rayleigh fading channel with uniform power delay profile is assumed.

The throughput is measured by changing the MT's location randomly to find the CDF of the throughput for $(N_{dan}, N_{mt})=(2,2)$. Independent fading is assumed for each retransmission. The spatial distribution of the throughput is plotted in Fig. 16 for DAN and CN when the normalized transmit $E_s/N_0=5$ dB. It can be seen from Fig. 16 that DAN achieves higher throughput than CN (note that CN can achieve high throughput only near SPC). The cell edge throughput is about 3 bps/Hz higher with DAN than with CN.

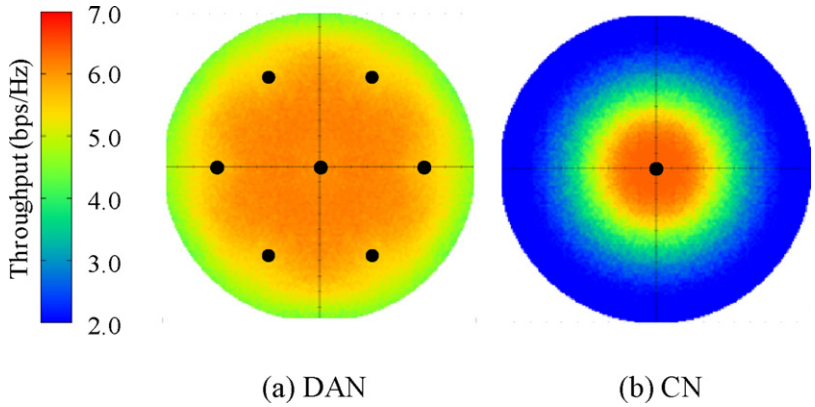

Fig. 16. Spatial distribution of throughput. (a) DAN. (b) CN.

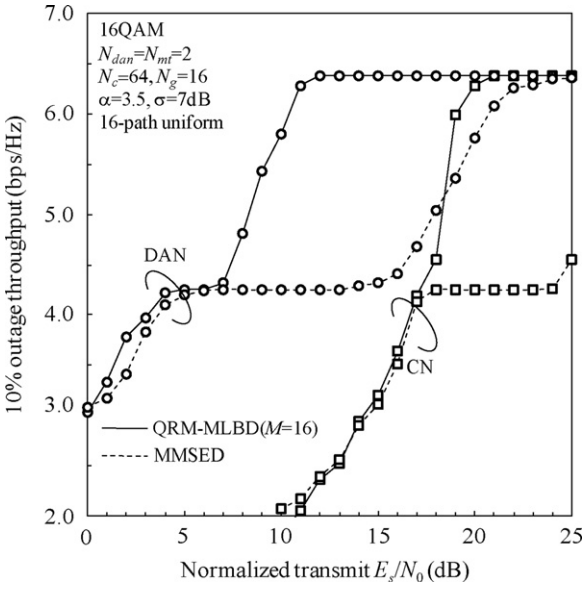

Fig. 17. 10%-outage throughput.

Fig. 17 plots the 10%-outage throughput for DAN and CN using QRM-MLBD. For comparison, the 10%-outage throughput is also plotted for DAN and CN using MMSE detection. DAN can reduce the normalized transmit E_s/N_0 required for achieving the same throughput as CN. The E_s/N_0 reduction from CN for a 10%-outage throughput of 5 bps/Hz is as much as about 10 dB. Furthermore, QRM-MLBD can improve the throughput compared to the MMSE detection. The E_s/N_0 reduction from MMSED for a 10%-outage throughput of 5 bps/Hz is as much as about 9 dB in DAN.

6. Conclusion

In this paper, we have investigated the potentiality of DAN combined with SC frequency-domain signal processing. Distributed SC-MIMO diversity, relay, beamforming, and multiplexing can solve the problems arising from the limited bandwidth, severe channel selectivity, and limited transmit power. It is desirable to use as many distributed antennas as possible while limiting the number of MT antennas to one or two so as to alleviate the complexity problem of MT. It was confirmed by the computer simulation that the DAN can be a promising future wireless network to provide gigabit wireless data services to mobile users. Theoretical analysis of SC-MIMO transmission performance of DAN is left as an important future study.

References

[1] Astély D, Dahlman E, Furuskär A, Jading Y, Lindström M, Parkvall S. LTE: the evolution of mobile broadband. IEEE Commun Mag 2009;47(April (4)):44–51.
[2] Falconer D, Ariyavistakul SL, Benyamin-Seeyar A, Eidson B. Frequency domain equalization for single-carrier broadband wireless systems. IEEE Commun Mag 2002;40(April (4)):58–66.
[3] Adachi F, Sao T, Itagaki T. Performance of multicode DS-CDMA using frequency domain equalization in a frequency selective fading channel. IEE Electron Lett 2003;39(January (2)):239–41.
[4] Adachi F, Takeda K, Obara T, Yamamoto T, Matsuda H. Recent advances in single-carrier frequency-domain equalization and distributed antenna network. IEICE Trans Fund 2010;E93-A(November (11)):2201–11.
[5] Tomeba H, Adachi F. Frequency-domain space-time block coded-joint transmit/receive diversity for the single carrier transmission. In: Proc. 10th IEEE international conference on communication systems (ICCS2006). 2006.
[6] Takeda K, Itagaki T, Adachi F. Application of space–time transmit diversity to single-carrier transmission with frequency-domain equalization and receive antenna diversity in a frequency-selective fading channel. IEE Proc Commun 2004;151(December (6)):627–32.
[7] Garg D, Adachi F. Throughput comparison of turbo-coded HARQ in OFDM, MC-CDMA and DS-CDMA with frequency-domain equalization. IEICE Trans Commun 2005;E88-B(February (2)):664–77.
[8] Laneman JN, Tse DNC, Wornell GW. Cooperative diversity in wireless networks: efficient protocols and outage behavior. IEEE Trans Inf Theory 2004;50(December (12)):3062–80.
[9] Nakada M, Takeda K, Adachi F. Channel capacity of SC-FDMA cooperative AF relay using spectrum division & adaptive subcarrier allocation. In: Proc IC-NIDC 2010. 2010. p. 579–83.
[10] Nakada M, Obara T, Yamamoto T, Adachi F. Direct/Cooperative AF relay switching using spectrum division/adaptive subcarrier allocation for SC-FDMA uplink. In: Proc APWCS 2011. 2011.
[11] Peng W, Adachi F. Frequency domain adaptive antenna array algorithm for single-carrier uplink transmission. In: Proc. IEEE personal, indoor and mobile radio communications symposium (PIMRC 2009). 2009. p. 1–5.
[12] Saleh A, Rustako A, Roman R. Distributed antennas for indoor radio communications. IEEE Trans Commun 1987;35(December (12)):1245–51.
[13] Yamamoto T, Takeda K, Adachi F. Training sequence-aided QRM-MLD block signal detection for single-carrier MIMO spatial multiplexing. In: Proc. IEEE international conference on communications (ICC 2011). 2011.
[14] Anderson JB, Mohan S. Sequential coding algorithms: a survey and cost analysis. IEEE Trans Commun 1984;32(February):169–76.